Int. J. Electrochem. Sci., 7 **(2012)** 12974 - 12982

International Journal of
ELECTROCHEMICAL
SCIENCE
www.electrochemsci.org

Short Communication

Investigation on the Property Degradation of Nickel-Base Alloy 825 in High Pressure H_2S Environments

S.Q. Zheng[1,*], *D.N. Wang*[1], *Y.M. Qi*[2], *C.F. Chen*[1], *L.Q. Chen*[1]

[1] State Key Laboratory of Heavy Oil Processing and Department of Materials Science and Engineering, China University of Petroleum, Beijing 102249, China
[2] School of Materials Science and Engineering, Beijing University of Aeronautics and Astronautics, Beijing 100191, China
[*]E-mail: zhengsq09@163.com

Received: 12 October 2012 / *Accepted:* 5 November 2012 / *Published:* 1 December 2012

The effects of tensile rate and H_2S pressure on the tensile property of nickel-base alloy 825 in wet H_2S environments were investigated by the slow strain rate tensile test (SSRT) and scanning electron microscopy (SEM). The results show that the tensile property degradation of alloy 825 has no obvious difference between 0.1MPa and 2MPa H_2S environments at a low tensile rate of 10^{-5}mm/s. However, the tensile property degradation of nickel-based alloy 825 differed obviously between 0.1MPa and 2MPa H_2S environments at a high tensile rate of 10^{-4}mm/s. Results of SEM examination show that the fractures of the specimens exposed to 0.1MPa and 2MPa H_2S environment present the similar feature at the low tensile rate of 10^{-5}mm/s. The fractures differed remarkably as the tensile rate increased to 10^{-4}mm/s. The difference of tensile property of alloy 825 under the two conditions is discussed from the insight of the self-repairing capability of passive film.

Keywords: Slow strain rate test; H_2S environment; property degradation; self-repairing capability

1. INTRODUCTION

The accidents of oil and gas fields are often caused by H_2S corrosion, especially the corrosion failure problems of oil casing in high acidic gas fields, which is the biggest obstacle to the exploration and development of high acidic gas fields [1]. Thus, both domestic and overseas have been trying to develop high quality stainless steel and corrosion resistant alloy pipes. In addition, the corrosion behaviors of corrosion resistant alloy have been investigated extensively [2-5]. One of the related research achievements is that the nickel-based alloy possessing the excellent corrosion resistance, high temperature performance and mechanical properties is used as oil well casing and the equipment material.

Nickel-based alloy exhibits the excellent corrosion resistance because of the presence of the passive films, which can separate the matrix of nickel-based alloy from corrosion environments effectively [6-8]. However, the local corrosion could be formed on the surface of nickel-based alloy due to the following situation. The local passive film is damaged by corrosion media and the destructive power is greater than the self-repairing ability. In the presence of external force load, the stress corrosion cracking is prone to happen in the vicinity of the local corrosion. The corrosion behavior and mechanism of steel in wet H_2S environments has been investigated extensively during the past twenty years [9-12]. However, most studies focused on the hydrogen induced cracking and sulfide stress corrosion cracking of the steel. The mechanical property damage of steel in acid gas field has not been yet investigated systematically. The slow strain rate test (SSRT) is one of the most widely accepted test methods for the accelerated SCC testing of metal material [13]. Many investigators studied the effects of experimental parameters such as structure [14], electrochemical changes [15] on the stress corrosion cracking. Additionally, the SSRT is widely applied in studying the metal fracture failure problem. The variation of the strength, elongation and mechanical properties can be researched by the SSRT. Thus, the SSRT provides a kind of effective experimental method to evaluation the material performance and the development of novel materials.

Based on the aforementioned insights, this work evaluated the influence of tensile rate on the tensile properties of nickel-base alloy 825 in different H_2S pressure environments by SSRT method. Furthermore, the self-repairing capability of passive film was discussed in accordance with the SSRT results.

2. EXPERIMENTAL METHOD

Table 1. Experimental conditions of SSRT

Experimental conditions Numbers	P_{H2S}(MPa)	tensile rate (mm/s)
1	0	10^{-5}
2	0.1	10^{-5}
3	2	10^{-5}
4	0	10^{-4}
5	0.1	10^{-4}
6	2	10^{-4}

Alloy 825 is a typical nickel-based alloy which is applied in high acidic oil and gas fields. Chemical compositions of the material are as follows(wt%): C, 0.008; Si, 0.30; Mn, 0.80; P, 0.012; S, 0.001; Mo, 3.16; Cr, 22.44; Ni, 39.16; Fe, balance.. The dimensions of specimens for slow strain rate tensile tests were illustrated in literature [16]. The specimens were polished smoothly prior to the experiments. These specimens were then rinsed with deionized water and degreased with acetone. All solutions were prepared according to TM0284-2003 [17], solution A, and thus contained 5% sodium chloride and 0.5% acetic acid. All the tests were performed at 25 °C. The experimental conditions are shown in Table 1.

After the SSRT tests, the specimens were removed, cleaned with acetone and dried. Then, the gauge length, fracture diameter are measured. The fracture surfaces were analyzed by scanning electron microscopy (SEM).

3. RESULTS

3.1 Results of SSRT tests

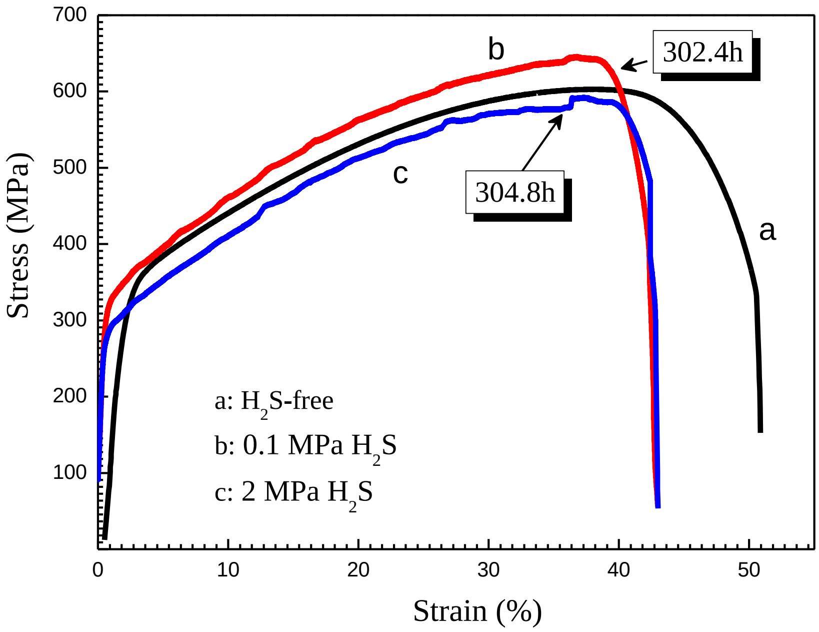

Figure 1. The stress-strain curves of nickel based alloy 825 in NACE-A solution at the tensile rate of 10^{-5}mm/s

Fig. 1 shows a series of stress-strain curves for nickel-based alloy 825 at the tensile rate of 10^{-5} mm/s. It can be seen that the strain of nickel based alloy 825 decreased from 51% to 43% in H_2S environment in comparison with that in H_2S-free environment. It indicated that the mechanical property was subjected to a certain degree of degradation in H_2S environment. In addition, the strain and time to failure have no obvious difference in the environments with different pressure of H_2S. It suggested that the mechanical property degradation of nickel-based alloy 825 differed little at the tensile rate of 10^{-5} mm/s.

Fig. 2 shows the stress-strain curve of nickel-based alloy 825 at the tensile rate of 10^{-4} mm/s. In contrast to the stress–strain curve of specimen in H_2S-free environment, the strain of nickel based alloy 825 decreased in the environment containing H_2S. Additionally, effect of H_2S pressure on the strain of nickel based alloy 825 is obvious at the tensile rate of 10^{-4}mm/s. The strain decreased from 41.5% to 35.8% as H_2S pressure increased from 0.1 MPa to 2 MPa. Furthermore, time to failure decreased from 29.28 h to 25.35 h when H_2S pressure increased from 0.1 MPa to 2 MPa. According to these results, it suggests that influence of H_2S pressure on the mechanical property degradation of nickel-based alloy 825 was obvious. Another phenomenon observed in Fig. 2 was that the strength of alloy 825 in 2MPa H_2S environment was higher than that in 0.1MPa H_2S environment.

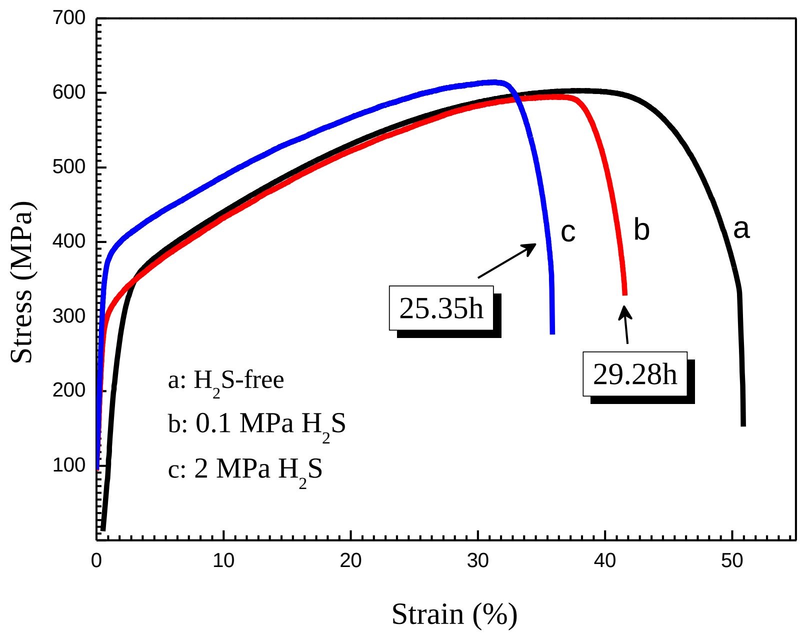

Figure 2. The stress-strain curves of nickel based alloy 825 in NACE-A solution at the tensile rate of 10^{-4}mm/s

Based on the aforementioned results, it was found that the mechanical properties of alloy 825 were dependent on the tensile rate in the H_2S environment. It is well known that the excellent corrosion resistance property of nickel-based alloy is attributed to the passive films with dense Cr, Ni, Mo oxide formed on the steel surface. Once the passive film was destroyed, the steel would be prone to local corrosion easily that may lead to crack nucleation and propagation. During the SSRT testing, the integrality of the passive film of nickel-based alloy could be destroyed as the stress and strain increased. When the tensile rate is 10^{-4}mm/s, the passive film is easy to be destroyed and it is also difficult to be self-repairing after destroyed. As a result, the steel matrix was exposed to the corrosive environment. Hydrogen atoms produced by the catholic reduction of the proton (H^+) could diffuse into the steel. The H enrichment in metal cooperated with the loading stress aggravated the degradation of the properties of alloy 825. Because of higher concentration of hydrogen in 2MPa H_2S solution, more hydrogen atoms could penetrate into the steel with the help of concentration gradient. Thus, the property degradation of nickel based alloy 825 in 2MPa H_2S environment is more serious than that in 0.1MPa H_2S environment. When the tensile rate decreased to 10^{-5} mm/s, the self-repairing capability of the passive films could be larger than the destroyed capability. As a result, the passive film after destroyed can repair rapidly due to the good self-repairing performance. Thus, there is no obvious difference in tensile property degradation between 0.1MPa and 2MPa H_2S environments for nickel based alloy 825, as shown in Fig. 1.

3.2 Analysis of fracture morphology

The fracture morphology of nickel-based alloy 825 exposed to different H_2S pressure environments at the tensile rate of 10^{-5} mm/s was shown in Fig. 3. It can be seen that the necking around the fracture of the specimens subjected to the environments with different pressure of H_2S is obvious, as shown in Fig. 3a, b, d and e.

A **B** **C**

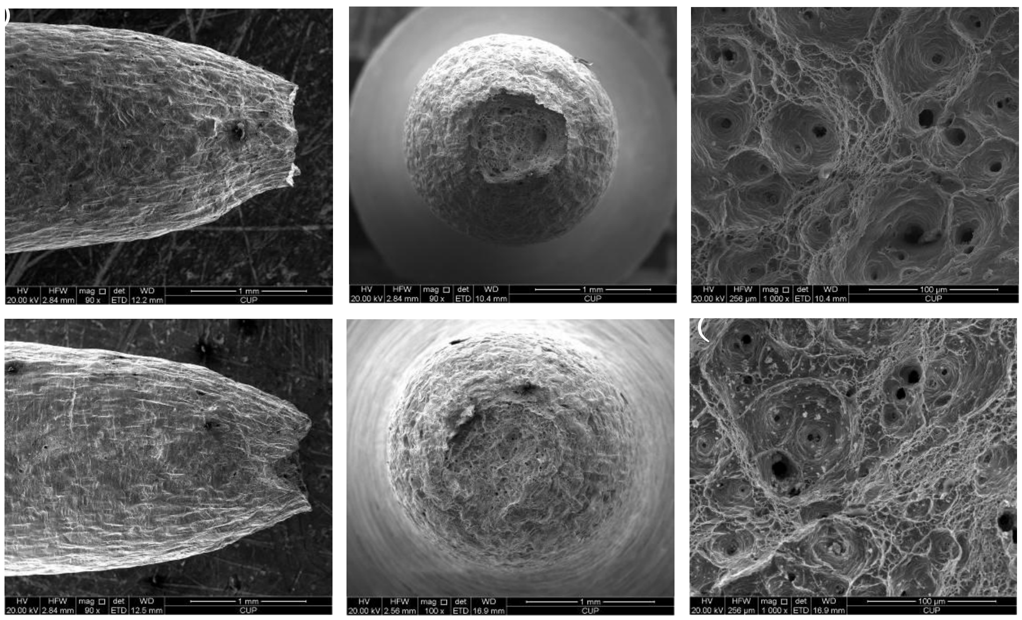

D **E** **F**

Figure 3. Fracture morphology of nickel based alloy 825 at the tensile rate of 10^{-5}mm/s (a) the longitudinal sections, 0.1MPa H_2S; (b) transect of fracture, 0.1MPa H_2S; (c) microcosmic morphology of fracture, 0.1MPa H_2S; (d) the longitudinal sections, 2MPa H_2S; (e) transect of fracture, 2MPa H_2S; (f) microcosmic morphology of the fracture, 2MPa H_2S

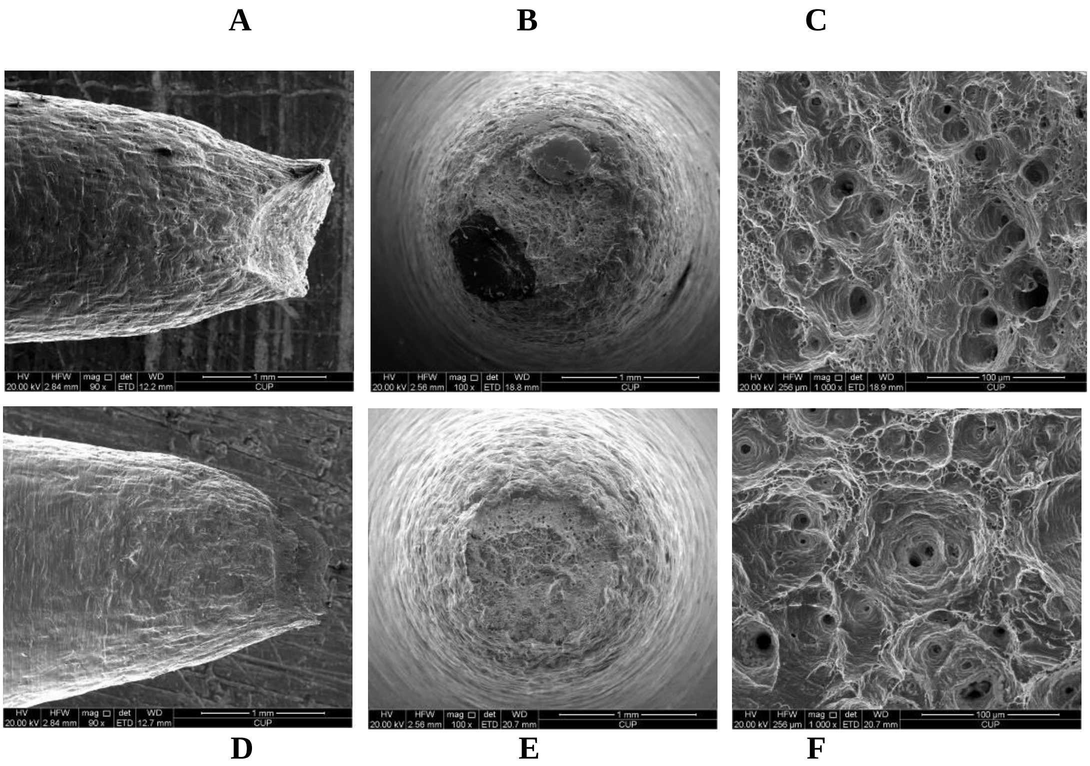

Figure 4. Fracture morphology of nickel based alloy 825 at the tensile rate of 10^{-4}mm/s. (a) the longitudinal sections, 0.1MPa H_2S; (b) transect of fracture, 0.1MPa H_2S; (c) microcosmic morphology of fracture, 0.1MPa H_2S; (d) the longitudinal sections, 2MPa H_2S; (e) transect of fracture, 2MPa H_2S; (f) microcosmic morphology of fracture, 2MPa H_2S

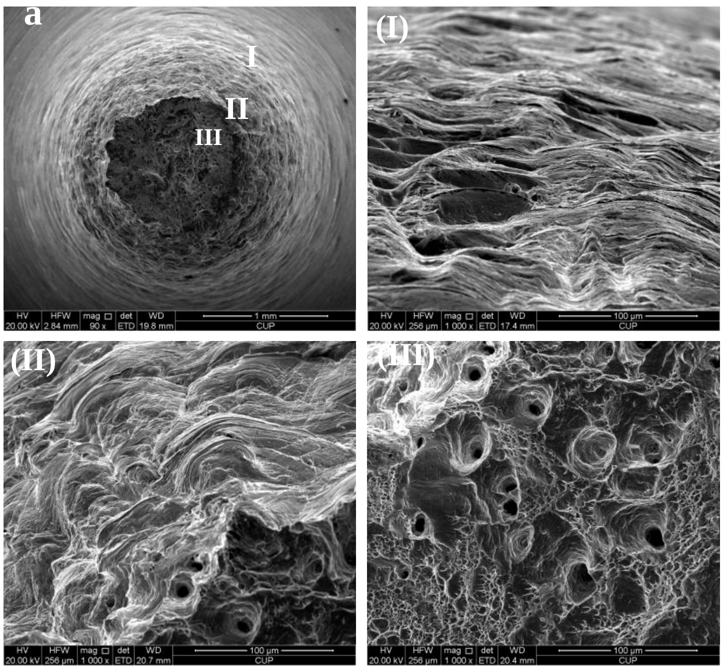

Figure 5. Fracture morphology of nickel based alloy 825 at the tensile rate of 10^{-4}mm/s in 2MPa H_2S environment. (I), (II), (III): The enlarged images of the signified region in image (a).

From the microcosmic morphology of the fracture, both the fracture surfaces exhibited dimple fractures (Fig. 3c and f), which is typical ductile fracture.

These findings indicated that nickel-based alloy 825 possesses good plasticity and toughness even in the H_2S environments. In addition, there is little difference in the morphology between 0.1MPa and 2MPa H_2S environments, indicative of the same property of nickel-based alloy 825 under two different H_2S pressures environments, which is consistent with the result of slow tensile stress strain curve (Fig. 1).

Fig. 4 shows the fracture morphology of nickel-based alloy 825 exposed to different H_2S pressure environments at the tensile rate of 10^{-4} mm/s. It can be seen that the necking phenomenon also existed in the vicinity of the fracture, indicative of the high-ductility in the nickel-based alloy 825. Compare Fig. 4a with Fig. 4d, it was found that the reduction of area of the fracture in 0.1MPa H_2S environment is larger than that in 2MPa H_2S environment.

In addition, the dimples in 0.1MPa H_2S environment are more and deeper than that in 2MPa H_2S environment. It suggests that the tensile property damage of nickel-based alloy 825 in 2MPa H_2S environment is more serious than that in 0.1MPa H_2S environment, which is consistent with the result of slow tensile stress strain curve in Fig. 2.

Fig. 5 shows the detail fracture morphology of nickel-based alloy 825 exposed to 2MPa H_2S environment at the tensile rate of 10^{-4}mm/s. Fig. 5I, II and III are the enlarged images of the indicated region in the image Fig. 5a. The region marked I is the edge of the fracture. The morphology in Fig. 5I exhibited river-like pattern. Furthermore, the river-like pattern became coarse near the fracture. The direction of the river coarsens is the direction of crack propagation. It suggested that the crack initiated in the surface of the alloy and propagated to the interior. The region marked II is the shear lip and the related microcosmic morphology is similar to that in the region marked I. The region marked III composed of some dimples.

4. DISCUSSION

Nickel-based alloy 825 is a kind of Ni-Fe-Cr alloy which is added with Mo, Cu and Ni and exhibits excellent resistance to acid corrosion and stress corrosion cracking. Meanwhile, nickel-based alloy 825 has good characteristics of local corrosion resistance, such as pitting corrosion and crevice corrosion.

During the SSRT tests, tensile stress can lead to the local rupture of the passive film, resulting in the local area exposed to the corrosive environment. The ruptured area would be dissolved in the H_2S environment. However, the ruptured area will suffer the passivation process due to the formation of the new passive film. As the stress increased, the passive film of the dissolved area could be destroyed again, resulting in the instantaneous dissolution of the steel again. This cycle process of passive film rupture, metal dissolution, and passivation again lead to the nucleation and propagation of stress corrosion cracks [18, 19].

According to the sliding dissolve model, it is known that the stress corrosion rate is the result of the match between the rupture rate and self-repairing rate of the passive film [20]. In the slow strain rate tensile tests, the rupture rate of the passive film is lower than the self-repairing rate of the passive film at a low tensile rate (such as 10^{-5} mm/s). The stress corrosion cracking susceptibility is low even in 0.1MPa and 2MPa H_2S environments. Therefore, the tensile property degradation of nickel-based alloy 825 differed little, as shown in Figs. 2 and 4. However, when the tensile rate increased to 10^{-4} mm/s, the rupture rate became higher than the self-repairing rate of the passive film. The self-repairing capability of the passive films was inhibited. The stress corrosion susceptibility increased. Thus, the tensile property degradation of nickel-based alloy 825 differed obviously between 0.1MPa and 2MPa H_2S environments, as shown in Figs. 3 and 5. According to the above analysis, it can be concluded that the self-repairing capability of the passive film of corrosion resistant alloy plays an important role in the tensile property in the H_2S environments.

5. CONCLUSIONS

(1) At a low tensile rate of 10^{-5} mm/s, there was no obvious difference in the tensile property degradation of nickel-based alloy 825 between 0.1MPa and 2MPa H_2S environments.

(2) At a high tensile rate of 10^{-4} mm/s, the tensile property degradation of alloy 825 presents an obvious difference between 0.1MPa and 2MPa H_2S environments. In addition, time to failure decreased from 29.28 h to 25.35h as H_2S pressure increased from 0.1MPa to 2MPa.

(3) The self-repairing capability of the passive film and the effect of hydrogen play a great influence on the tensile properties of nickel-base alloy 825 in the H_2S environment.

ACKNOWLEDGEMENTS
This work was financially supported by the Natural Science Foundation of China (No. 51271201 and No.51171208) and the Science Foundation of China University of Petroleum, Beijing (No. LLYJ-2011-41).

References

1. R. Nishimura, Y. Maeda, *Corros. Sci.,* 46(2004)769.
2. S. Zheng, Y. Kuang, C. Chen, *Nanosci. Nanotech. Let.,* 3(2011)204.
3. S. Zheng, C. Zhou, C. Chen. *Rare Metal Mat. Eng.*, 41(2012)256.
4. Y. Li, F. Wu, *Thin Solid Films*, 24(2010)7527.
5. Z. Yin, W. Zhao, Z. Bai, Y. Feng and W. Zhou, *Electrochim. Acta*, 53(2008)3690.
6. R. Jiang, C. Chen, S. Zheng. *Electrochim. Acta*, 55 (2010) 2498.
7. R. Jiang, C. Chen, S. Zheng, L. Cui. *J. Electroanal. Chem.*, 658 (2011) 52.
8. J. Schultze, M. Lohrengel. *Electrochim. Acta*, 45(2000)2499.
9. M. Lucio-Garcia, J. Gonzalez-Rodriguez, M. Casales, *Corros. Sci.*, 51 (2009) 2380.
10. S. Zheng, C. Li, C. Chen, *Metallofiz. Nov. Tekh+.*, 34(2012)57.

11. T. Jin, Z. Liu, Y. Cheng, *Int. J. Hydrogen Energy*, 35 (2010) 8014.
12. Y. Yao, X. Pang, K. Gao, *Int. J. Hydrogen Energy*, 36 (2011) 5729.
13. J. Deleume, D. Poquillon, V. Garat, J. Cloue and E. Andrieu, *Corros. Sci.*, 50(2008)737.
14. Z. Lu, T. Shoji, F. Meng, H. Xue, Y. Qiu, Y. Takeda and K. Negishi, *Corros. Sci.*, 53(2011)1916.
15. A. Torres-Islas, J. Gonzalez-Rodriguez, *Int. J. Electrochem. Sci.*, 4(2009)640.
16. S. Zheng, Y. Qi, C. Chen, S. Li, *Corros. Sci.*, 60(2012)59.
17. NACE standard TM0284-2003. NACE International, Houston, Texas, 2003.
18. S. El-egamy, W. Badway. *J. Appl. Electrochem.*, 34(2004)15.
19. C. Lee, *Int. J. Electrochem. Sci.*, 7(2012) 8487.
20. Y. Wang, M. Kanedome, T. Yasuda T. Suda, S. Watanabe, S. Ohnuki, T. Nagasaka and T. Muroga, *J. Nucl. Mater.*, 329(2004)477.